Supporting Information

Boosting the Catalytic Performance of Iron Phosphide Nanorods for the Oxygen Evolution Reaction by Incorporation of Manganese.

*Da Li, Habib Baydoun, Bogdan Kulikowski, Stephanie L. Brock**

Department of Chemistry, Wayne State University, Detroit, Michigan 48202, United States

Stephanie L. Brock

*Email: sbrock@chem.wayne.edu

Faradaic Efficiency Calculation:

	% O_2	% N_2	Ratio
Air	20.3	79.7	r_{air} = 0.2547
Blank	21.2	78.8	r_{blank} = 0.2690
$Fe_{1.1}Mn_{0.9}P$	27.0	73.0	r_{CoMnP} = 0.3699

Head space volume = 10.4 mL

Volume of solution = 35.7 mL

Henry's law constant (K) = 769.23 $\frac{L.atm}{mol}$

nO_2 in head space before catalysis (A) = 90.5 µmol for 10.4 mL

O_2 produced in headspace = $\frac{r_{lb}-r_{blank}}{r_{air}} \times A = \frac{0.3699-0.2690}{0.2547} \times 90.4 = 35.8\ \mu mol$

O_2 dissolved = nO_2 final – nO_2 initial

$= \frac{p_{O2\ final}}{K} * V_{solution} - \frac{p_{O2\ initial}}{K} * Vs_{olution}$

$= (0.297\text{-}0.203)(\frac{35700\ \mu L}{769.23(\frac{L.atm}{mol})}) = 4.4\ \mu mol$

Total amount of O_2 produced = n_{O2} in headspace + n_{O2} dissolved

$=35.8 + 4.4$

$= 40.2\ \mu mol$

n O_2 based on charge = $\frac{Q_{LB}-Q_{blank}}{4\times 0.096485} = \frac{18.07-1.72}{4\times 0.096485} = 42.4\ \mu mol$

Faradaic efficiency = $\frac{n_{O2\ experimental}}{n_{O2\ charge}} \times 100 = \frac{40.2}{42.4} \times 100 = 95\ \%$

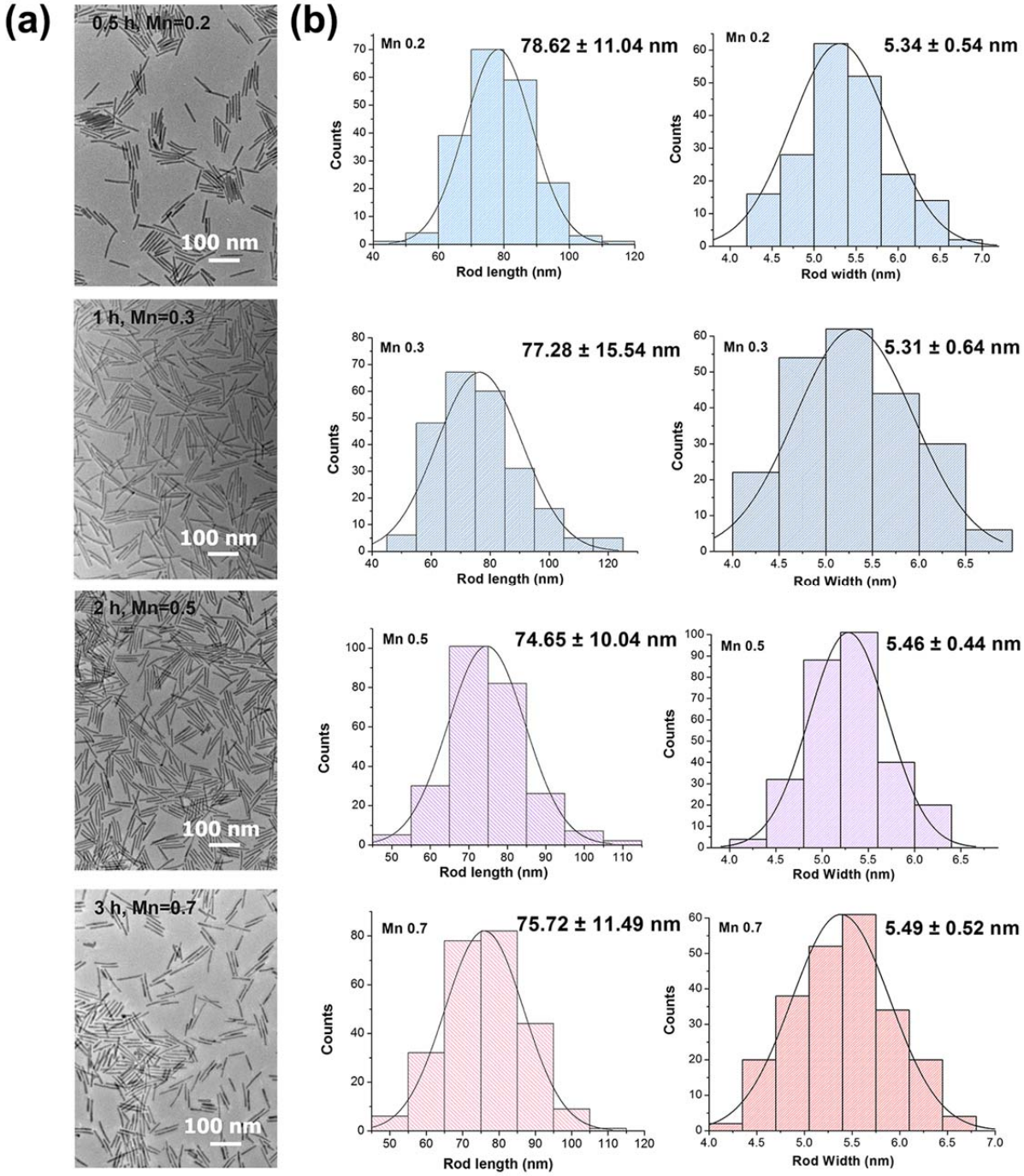

Figure S1. (a) TEM images of $Fe_{2-x}Mn_xP$ nanorods as a function of time (targeted ratio Fe/Mn = 0.75/1.25). (b) Histograms for the rod length and width distribution (measured from TEM) for different compositions of $Fe_{2-x}Mn_xP$. The Mn composition indicated was determined by ICP-MS (Table S1).

Table S1. Composition analysis (from EDS and ICP analysis) of $Fe_{2-x}Mn_xP$ nanorods prepared from a Mn/Fe ratio of 1.25/0.75 at 320 ºC.

Reaction time (h)	Actual ratio from EDS (Mn : Fe)	Actual ratio from ICP (Mn : Fe)
0.5	0.21 : 1.79	0.20 : 1.80
1	0.31 : 1.69	0.32 : 1.68
2	0.48 : 1.52	0.49 : 1.51
3	0.70 : 1.30	0.71 : 1.29
6	0.71 : 1.29	0.73 : 1.27
10	0.69 : 1.31	0.71 : 1.29
5 (2^{nd} injection)	0.92 : 1.08	0.91 : 1.09

Table S2. Target compositions and product compositions (from EDS) of $Fe_{2-x}Mn_xP$ nanoparticles after 2 h reaction.

Starting ratio (Mn : Fe)	Actual ratio from EDS (Mn : Fe)
1.0 : 1.0	0.36 : 1.64
1.25 : 0.75	0.48 : 1.52
1.4 : 0.6	0.48 : 1.52
1.5 : 0.5	0.55 : 1.45

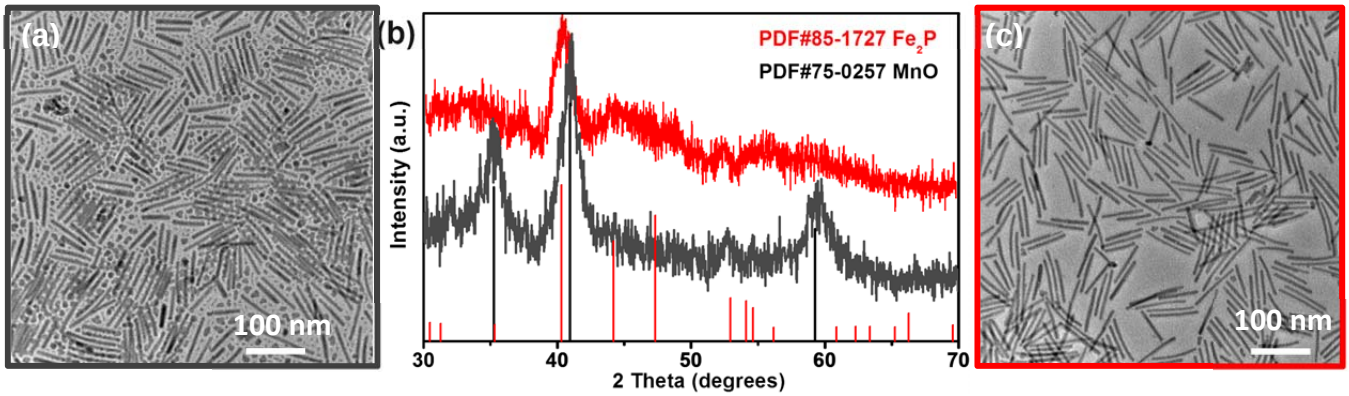

Figure S2. (a) TEM image and (b) PXRD pattern of the product after 10 h reaction (grey) and the product after size-selective precipitation (red). (c) TEM image of the product after size-selective precipitation to remove the small, spherical MnO nanoparticles.

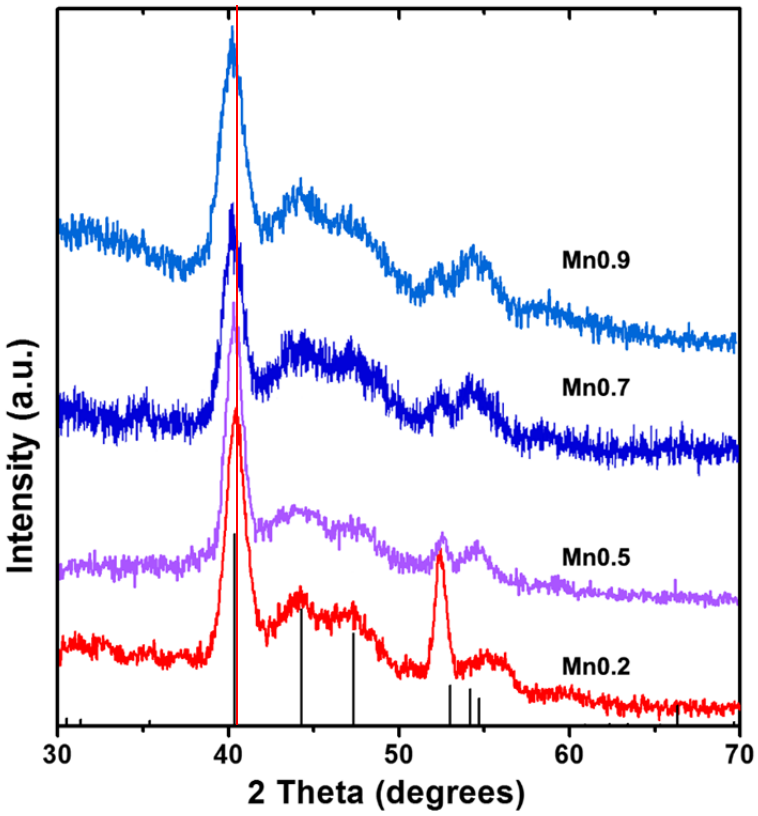

Figure S3. PXRD pattern of different compositions of $Fe_{2-x}Mn_xP$ nanorods, revealing a shift in the (111) reflection (ca 40° 2θ) to lower angle with increasing x.

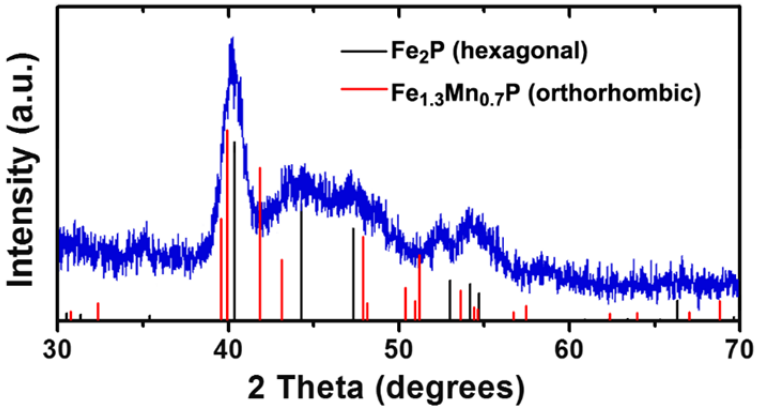

Figure S4. PXRD pattern of $Fe_{1.3}Mn_{0.7}P$ nanorods. Reference patterns are for hexagonal Fe_2P (PDF # 85-1727) and orthorhombic $Fe_{1.3}Mn_{0.7}P$ (simulated).[1]

Table S3 Comparison of the OER activities of the $Fe_{1.1}Mn_{0.9}P$ catalysts reported here in alkaline conditions with recently published results.

Materials	Overpotential at 10 mA cm^{-2} (mV)	Electrolyte	Main Paper Reference[SI reference]
IrO_2	320	1 M KOH	3[2]
IrO_2	360	1 M KOH	9[3]
IrO_2	470	0.1 M KOH	37[4]
CoP nanorods/C (0.71 mg/cm^2)	340	1 M KOH	11[5]
CoP nanoparticles/C (0.71 mg/cm^2)	320	1 M KOH	11[5]
Ni_2P nanowires/FTO (~0.10 mg/cm^2)	400	1 M KOH	7[6]
Ni_2P nanoparticles/FTO (~0.10 mg/cm^2)	500	1 M KOH	7[6]
FeP@Au nanoparticles (0.2 mg/cm^2)	320	1 M KOH	39[7]
NiCoP/rGO hybrids (0.15 mg/cm^2)	270	1 M KOH	40[8]
CoFeP (~0.57 mg/cm^2)	370	0.1 M KOH	14[9]
CoP/C (0.40 mg/cm^2)	360	0.1 M KOH	38[10]
CoP hollow polyhedrons (~0.10 mg/cm^2)	400	1 M KOH	13[11]
CoMnP (0.28 mg/cm^2)	330	1 M KOH	20[12]
$Fe_{1.1}Mn_{0.9}P$ nanoparticles (0.28 mg/cm^2)	350	1 M KOH	This work

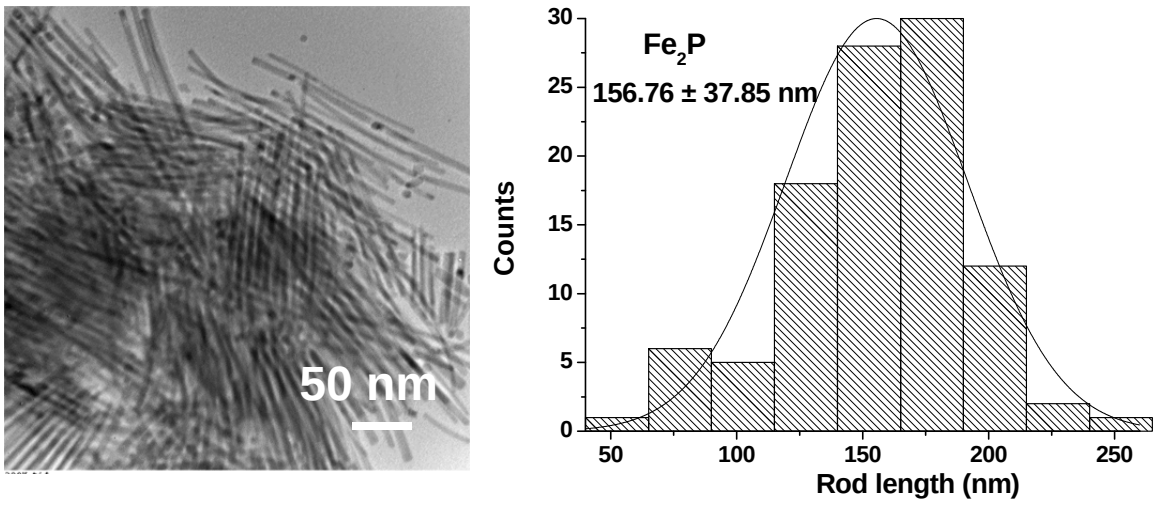

Figure S5. (a) TEM images of Fe_2P nanorods and histograms for the rod length distribution (measured from TEM).

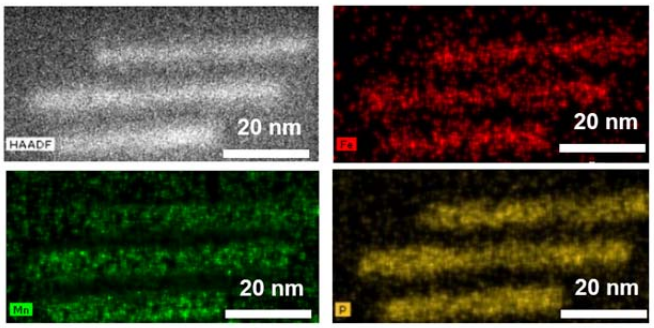

Figure S6. HAADF image and its corresponding STEM elemental mapping data for $Fe_{1.1}Mn_{0.9}P$ nanorods.

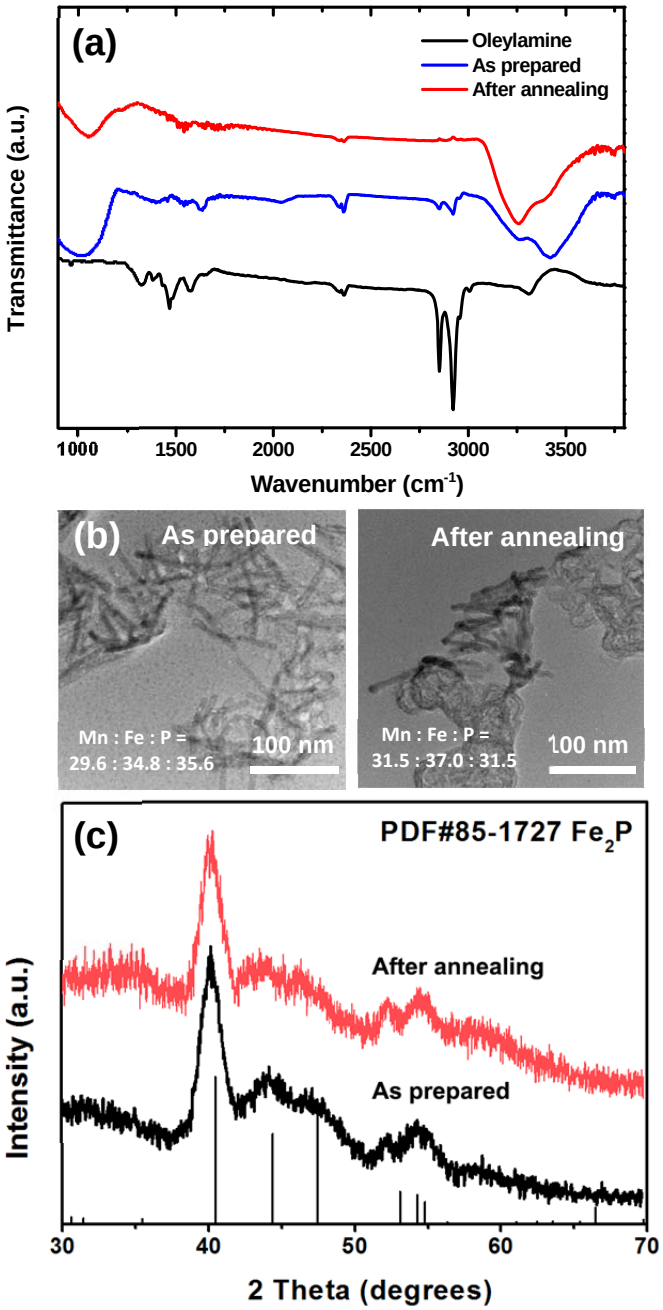

Figure S7. (a) FT-IR spectra of oleylamine and $Fe_{1.1}Mn_{0.9}P$/C nanorods, revealing the existence of both oleylamine ligand and phosphate on the surface of FeMnP nanorods (C-H stretch: 2852 and 2924 cm^{-1}; C-N stretch: 1385 cm^{-1}; N-H stretch: 3250-3450 cm^{-1}; P=O stretch: 1000-1050 cm^{-1}); (b) TEM images (element ratios measured from EDS) and (c) XRD patterns of $Fe_{1.1}Mn_{0.9}P$/C nanorods before and after annealing. The low-contrast curved features in the annealed sample (b) are ascribed to residual carbon black.

Table S4 ICP-MS data of the electrolyte solution before and after a fifteen-hour controlled potential electrolysis (CPE) experiment, which was carried out in 1.0 M KOH, by applying a constant potential of 1.58 V (vs RHE).

Element	Before (5 h soak) Concentration (ppb)	After CPE Concentration (ppb)	After CPE (Mole change ratio x : Mn)
P K	11.6	208.84	24.27
Mn K	2.08	16.50	1
Fe K	22.32	42.51	1.38

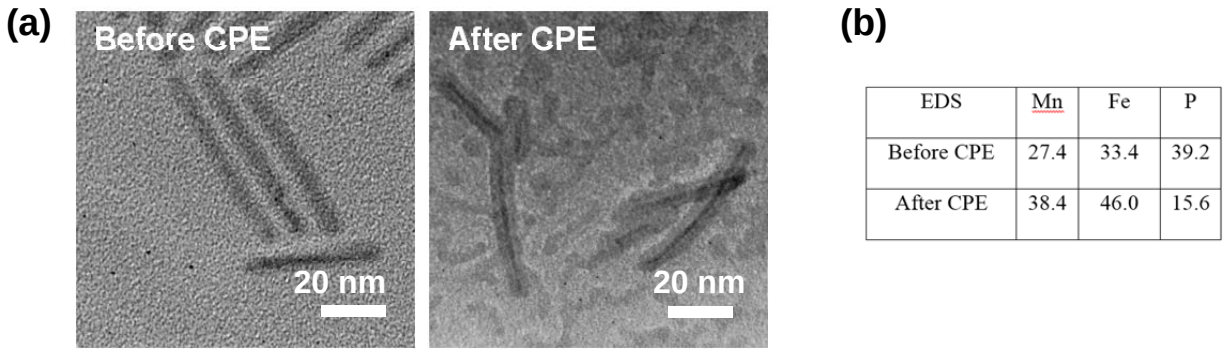

EDS	Mn	Fe	P
Before CPE	27.4	33.4	39.2
After CPE	38.4	46.0	15.6

Figure S8. TEM images of $Fe_{1.1}Mn_{0.9}P$ nanorods before and after CPE.

References

1. Fruchart, R.; Roger, A.; Sendteur, J. P., Crystallographic and Magnetic Properties of Solid Solutions of Phosphides M_2P M=Cr Mn Fe Co and Ni. *J. Appl. Phys.* **1969,** *40*, 1250-1257.
2. McCrory, C. C. L.; Jung, S.; Peters, J. C.; Jaramillo, T. F., Benchmarking Heterogeneous Electrocatalysts for the Oxygen Evolution Reaction. *J. Am. Chem. Soc.* **2013,** *135*, 16977-16987.
3. Dutta, A.; Samantara, A. K.; Dutta, S. K.; Jena, B. K.; Pradhan, N., Surface-Oxidized Dicobalt Phosphide Nanoneedles as a Nonprecious, Durable, and Efficient OER Catalyst. *ACS Energy Lett.* **2016,** *1*, 169-174.

4. Lee, Y.; Suntivich, J.; May, K. J.; Perry, E. E.; Shao-Horn, Y., Synthesis and Activities of Rutile IrO_2 and RuO_2 Nanoparticles for Oxygen Evolution in Acid and Alkaline Solutions. *J. Phys. Chem. Lett.* **2012,** *3*, 399-404.
5. Chang, J.; Xiao, Y.; Xiao, M.; Ge, J.; Liu, C.; Xing, W., Surface Oxidized Cobalt-Phosphide Nanorods As an Advanced Oxygen Evolution Catalyst in Alkaline Solution. *ACS Catal.* **2015,** *5*, 6874-6878.
6. Han, A.; Chen, H. L.; Sun, Z. J.; Xu, J.; Du, P. W., High catalytic activity for water oxidation based on nanostructured nickel phosphide precursors. *Chem. Commun.* **2015,** *51*, 11626-11629.
7. Masud, J.; Umapathi, S.; Ashokaan, N.; Nath, M., Iron phosphide nanoparticles as an efficient electrocatalyst for the OER in alkaline solution. *J. Mater. Chem. A* **2016,** *4*, 9750-9754.
8. Li, J.; Yan, M.; Zhou, X.; Huang, Z.-Q.; Xia, Z.; Chang, C.-R.; Ma, Y.; Qu, Y., Mechanistic Insights on Ternary $Ni_{2-x}Co_xP$ for Hydrogen Evolution and Their Hybrids with Graphene as Highly Efficient and Robust Catalysts for Overall Water Splitting. *Adv. Funct. Mater.* **2016,** *26* , 6785-6796.
9. Mendoza-Garcia, A.; Zhu, H. Y.; Yu, Y. S.; Li, Q.; Zhou, L.; Su, D.; Kramer, M. J.; Sun, S. H., Controlled Anisotropic Growth of Co-Fe-P from Co-Fe-O Nanoparticles. *Angew. Chem. Int. Ed.* **2015,** *54*, 9642-9645.
10. Ryu, J.; Jung, N.; Jang, J. H.; Kim, H. J.; Yoo, S. J., In Situ Transformation of Hydrogen-Evolving CoP Nanoparticles: Toward Efficient Oxygen Evolution Catalysts Bearing Dispersed Morphologies with Co-oxo/hydroxo Molecular Units. *ACS Catal.* **2015,** *5*, 4066-4074.
11. Liu, M.; Li, J., Cobalt Phosphide Hollow Polyhedron as Efficient Bifunctional Electrocatalysts for the Evolution Reaction of Hydrogen and Oxygen. *ACS Appl. Mater. Interfaces* **2016,** *8*, 2158-2165.
12. Li, D.; Baydoun, H.; Verani, C. N.; Brock, S. L., Efficient Water Oxidation Using CoMnP Nanoparticles. *J. Am. Chem. Soc.* **2016,** *138*, 4006-4009.